

Mitochondrial Dysfunction by Complex II Inhibition Delays Overall Cell Cycle Progression Via Reactive Oxygen Species Production

Hae-Ok Byun,¹ Hee Young Kim,¹ Jin J. Lim,¹ Yong-Hak Seo,^{1,2} and Gyesoon Yoon^{1,2*}

¹Department of Biochemistry and Molecular Biology, Ajou University School of Medicine, Suwon 443-721, South Korea

²Department of Molecular Science & Technology (BK21), The Graduate School, Ajou University, Suwon 443-721, South Korea

Abstract Mitochondrial complex II defect has recently been implicated in cellular senescence and in the ageing process of which a critical phenotype is retardation and arrest of cellular growth. However, the underlying mechanisms of how complex II defect affects cellular growth, remain unclear. In this study, we investigated the effect of complex II inhibition using a subcytotoxic dose (400 μ M) of 2-thenoyltrifluoroacetone (TTFA), a conventional complex II inhibitor, on cell cycle progression. TTFA (400 μ M) directly decreased KCN-sensitive cellular respiration rate to 67% of control and disrupted the mitochondrial membrane potential. In contrast to other respiratory inhibitors such as rotenone, antimycin A, and oligomycin, TTFA prolonged the duration of each phase of the cell cycle (G1, S, and G2/M) equally, thereby delaying overall cell cycle progression. This delay was accompanied by a biphasic increase of reactive oxygen species (ROS) and concurrent glutathione oxidation, in addition to a slight decrease in the cellular ATP level. Finally, the delay in cell cycle progression caused by TTFA was proved to be mainly due to ROS overproduction and subsequent oxidative stress, as evidenced by its reversal following pretreatment with antioxidants. Taken together, these results suggest that an overall delay in cell cycle progression due to complex II defects may contribute to ageing and degenerative diseases via inhibition of cellular growth and proliferation without arrest at any specific phase of the cell cycle. *J. Cell. Biochem.* 104: 1747–1759, 2008. © 2008 Wiley-Liss, Inc.

Key words: complex II; 2-thenoyltrifluoroacetone; cell cycle delay; mitochondrial respiration; reactive oxygen species

Mitochondrial oxidative phosphorylation is the main source of ATP production in aerobically growing eukaryotic cells. Five membrane-

anchored protein complexes (complex I–V) are involved in mitochondrial oxidative phosphorylation, and defects in this process have been implicated in the progression of ageing and in diverse age-related disorders such as cancer and degenerative diseases [Wallace, 1999, 2005; Lesnefsky and Hoppel, 2006]. In addition to their main role in ATP generation, mitochondria are known to modulate intrinsic apoptotic initiation and be a major generator of reactive oxygen species (ROS) [Liu et al., 1996; Papa and Skulachev, 1997; Ishiguro et al., 2001]. Thus, it has been broadly accepted that there is a close relationship between respiratory control and mitochondrial apoptotic initiation and oxidative stress, two critical events in diverse age-related pathogenesis.

Mitochondrial complex II, also known as succinate-ubiquinone oxidoreductase, is a unique membrane-bound component of the Krebs cycle as well as part of the respiratory

This article contains supplementary material, which may be viewed at the Journal of Cellular Biochemistry website at <http://www.interscience.wiley.com/jpages/0730-2312/suppmat/index.html>.

Hae-Ok Byun and Hee Young Kim contributed equally to this work.

Grant sponsor: Korea Science and Engineering Foundation; Grant number: R13-2003-019-01004-0; Grant sponsor: Korea Research Foundation; Grant number: KRF-2004-205-C00181; Grant sponsor: Department of Medical Science, The Graduate School, Ajou University (2002 Research Grant).

*Correspondence to: Gyesoon Yoon, San 5, Wonchon-dong, Yontong-gu, Suwon 443-721, South Korea.

E-mail: ypeace@ajou.ac.kr

Received 5 November 2007; Accepted 29 January 2008

DOI 10.1002/jcb.21741

© 2008 Wiley-Liss, Inc.

chain, indicating its role as a metabolic linker of both processes. In contrast to other complexes, the intimate involvement of complex II defects has recently been focused in ageing and cancers such as hereditary paraganglioma and familial pheochromocytoma [Ishii et al., 1998; Baysal et al., 2000; Rustin and Rotig, 2002; Albayrak et al., 2003; Benn et al., 2003], implying that there is a specific mechanism modulated by complex II and that the defects in this process contribute to control cellular growth and proliferation. The most striking fact is that a mutation of cytochrome *b*, the third subunit of complex II, causes premature ageing in nematode [Ishii et al., 1998], suggesting its critical involvement as a causative factor in senescence process. Irreversible growth arrest and decreased cellular proliferation are key characteristics of the senescence process [Wallace, 1999]. However, the mechanism(s) by which complex II regulates cellular proliferation and cell cycle progression remains unclear.

Mitochondrial respiratory inhibitors are widely used to investigate the effects of respiratory defects on cellular function as detailed mechanisms of their inhibition are well defined [Nicholls and Ferguson, 2002]. Among the respiratory complexes, complexes I and II are priming enzymes for respiration that accept electrons from NADH and succinate, respectively, suggesting that they may have similar effect on cellular function. However, while there are several reports that the complex I inhibitor, rotenone, leads to G2/M cell cycle arrest, apoptosis, and other related neurotoxicities [Isenberg and Klauing, 2000; Armstrong et al., 2001; Li et al., 2003], little has been published on the effects of the complex II inhibitor, 2-thenoyltrifluoroacetone (TTFA). In addition, the respiratory inhibitors have generally been reported to induce apoptosis through cytochrome *c* release and most studies using the inhibitors have been focused to elucidate the mechanisms involved in the apoptotic process [Wolvetang et al., 1994; Nishimura et al., 2001]. However, to understand the mechanism(s) related to senescence-associated modulation of cellular growth and cell cycle progression, it is essential to elucidate the subcytotoxic effect of the respiratory inhibitors on these processes, which has rarely been reported. We report here that the mitochondrial respiratory defect induced by subcytotoxic dose of TTFA results in an overall delay in cell cycle progression, which is quite different from the effects of other mitochondrial

complex inhibitors. We also demonstrate that ROS and subsequent oxidative stress is the major mechanism involved in the delay of cell cycle progression caused by complex II defect.

MATERIALS AND METHODS

Cell Culture and Growth Rates

Chang cells were obtained from the American Type Culture Collection (Manassas, VA) and cultured in Dulbecco's modified Eagle's medium (DMEM; GibcoBRL, Gaithersburg, MD) or DMEM (high glucose) supplemented with 10% (v/v) fetal bovine serum (FBS; GibcoBRL) in a 37°C incubator with 5% CO₂ in air. Cells (5×10^5) were seeded into 100 mm culture plates, cultured in DMEM containing 10% FBS for 24 h, and challenged with 2-thenoyltrifluoroacetone (TTFA; Sigma, St. Louis, MO) for the indicated periods. To estimate the growth rates, cells were harvested by trypsinization, and counted with a hemocytometer after staining with 0.4% (w/v) trypan blue (GibcoBRL) to exclude dead cells at the indicated times. No trypan blue-positive cells were observed until 72 h exposure to 400 μ M TTFA.

Cell Synchronization at the Late G1 Phase and Cell Cycle Analysis

Chang cells were synchronized at the late G1 phase by thymidine double treatment (0.5 mg/ml) for 18 h with an 8 h interval. Cells were released from synchronization by refreshing the medium in the absence or presence of 400 μ M TTFA, and collected at the indicated times. Cell cycle analysis was performed by propidium iodide (PI) staining with the CycleTESTTM PLUS DNA reagent kit (Becton Dickinson, Ontario, Canada), using the manufacturer's instructions. Briefly, cells were trypsinized, collected by centrifugation, washed and resuspended in PBS (137 mM NaCl, 2.7 mM KCl, 10 mM phosphate buffer, pH 7.4) before fixing in 70% ethanol at a density of 1×10^6 cells/ml. In keeping with the protocol, fixed cells were stained with 50 μ g/ml of PI for at least 10 min before flow cytometric analysis (Becton-Dickinson FACSsorter). The instrument was set to collect 1×10^4 cells, and the cell cycle profile analyzed using CELLQuest software. For analyzing the effects of TTFA on asynchronous cell cycle patterns, subconfluent cells were treated with TTFA for the indicated periods, and collected.

Determination of the Cellular ATP Level

Cellular ATP levels were measured with the bioluminescence assay using the ATP Determination Kit protocol (Molecular Probe Corp., Eugene, OR) as previously described [Yoon et al., 2003]. Briefly, cell lysates (5 μ g) were mixed with 100 μ l of luciferase reagent, and luminescence analyzed with 10 s integration on a luminometer (TD-20/20, Sunnyvale, CA). ATP levels of the samples were determined from a calibration curve of known ATP concentrations measured at the same time. ATP levels are expressed as pmol/ μ g of cellular lysate protein.

Determination of the Intracellular ROS Level and Mitochondrial Membrane Potential, and Visualization of Mitochondrial Morphology

To estimate the intracellular ROS content, we used two fluorogenic probes, 2',7'-dichlorodihydrofluorescein diacetate (DCFH-DA; Molecular Probe) and dihydrorhodamine 123 (DHR123; Molecular Probe). Cells were treated with TTFA for the indicated periods, and further incubated in media containing 10 μ M DCFH-DA or DHR123 for 15 min at 37°C. Stained cells were washed, resuspended in PBS, and analyzed by flow cytometry (FACS Vantage, Becton Dickinson Corp.).

To estimate mitochondrial membrane potential, cells were treated with TTFA for the indicated periods, further incubated in media containing 10 μ g/ml JC-1 (Molecular probe), and washed with PBS for 20 min at 37°C. The average cellular red and green fluorescence intensities were obtained by Axiovision 4.2 software with ratio module after visualization with 100 ms on Axiovert 200 M equipped with HBO103 using a LD Plan-Neofluar 40 \times objective (Carl Zeiss AG, Gottingen, Germany). The ratio of red fluorescence to green one was estimated and expressed as percentage of control.

To visualize the mitochondrial morphology, mtYFP-Chang cells [Yoon et al., 2006] were exposed to 400 μ M TTFA and the mitochondria were imaged on Axiovert 200M equipped with HBO103 using a Plan Apo 100 \times , 1.4 NA oil-immersion objective with 1.6 \times optovar (Carl Zeiss AG). To obtain electron microscopic images of the mitochondria, cells were fixed, sectioned, and stained as previously described [Yoon et al., 2006]. The stained cells were observed and photographed under transmission

electron microscope (Zeiss EM 902A, Leo, Oberkochen, Germany).

Endogenous Cellular Oxygen Consumption

Endogenous respiration was measured as described previously [Yoon et al., 2003]. Briefly, exponentially growing Chang cells (5×10^6) were cultured, washed with TD buffer (0.137 M NaCl, 5 mM KCl, 0.7 mM Na₂HPO₄, 25 mM Tris-HCl, pH 7.4), and collected by trypsinization. After resuspending the cells in 0.1 ml of complete medium without phenol red, the cells were transferred to the chamber of Mitocell equipped with Clark oxygen electrode (782 Oxygen Meter, Strathkelvin Instrument, Glasgow, UK). Oxygen consumption rates were measured to obtain maximum respiration rate, and its specificity for mitochondrial respiration was confirmed by adding 5 mM KCN. To measure the direct effect of TTFA on cellular respiration, the indicated doses of TTFA were added directly to the cells respiring in the chamber and the rate after exposure to TTFA was compared to the initial rate.

Intracellular GSH and GSSG Assays

Total glutathione (GSH) and oxidized glutathione (GSSG) levels were analyzed according to a previous protocol [Tietze, 1969]. Briefly, to determine the GSH level, cells were harvested and suspended in 1% sulfosalicylic acid, and the supernatant applied to the assay after removing aggregates by centrifuging at 8,000g for 10 min. The reaction was initiated by adding the supernatant (1 μ g) to a 96-well microtiter plate containing 200 μ l of assay mixture [125 μ M NaPO₄, pH 7.5, 0.3 mM NADPH, 6 mM 5, 5'-dithio-bis-(2-nitrobenzoic acid) (DNTB; Sigma), 0.12 U glutathione reductase (Sigma)]. Maximal reduction of DNTB by GSH was measured by monitoring absorption at 405 nm, and compared to the calibration curve obtained using standard GSH (Sigma) with a ThermoMax microplate reader (Molecular Devices Co., Sunnyvale, CA). To monitor the GSSG level, cells were treated with 2-vinylpyridine to modify pre-existing GSH, and the supernatant (50 μ g) subjected to the above protocol using standard GSSG (Sigma) to obtain the calibration curve.

Western Blot Analysis and Antibodies

Cells were washed twice with PBS and lysed with lysis buffer (50 mM Tris-Cl, pH 7.5, 0.1 M

NaCl, 1 mM EDTA, 1% Triton X-100, 10 $\mu\text{g}/\text{ml}$ each of aprotinin and leupeptin, and 1 mM PMSF). A portion (40 μg) of lysate was electrophoresed on SDS-polyacrylamide gel. The proteins were electrically transferred onto nitrocellulose membrane (Protran, S&S, Inc., NH) and subjected to immunoblot analysis using antibodies. The immunoblots were developed with the enhanced chemiluminescence system (ECL, Amersham Pharmacia Biotech.). Antibody against PARP (C2-10) was purchased from Zymed Laboratories, Inc. (Carlsbad, CA) and p16 antibody (554079) was from BD Biosciences (San Jose, CA). Antibodies against p21 (C-19) and p27 (N-20) were purchased from Santa Cruz Biotechnology, Inc. (Santa Cruz, CA).

RESULTS

Effects of Mitochondrial Respiratory Inhibitors on Cell Cycle Progression

To elucidate whether complex II inhibition by TTFA affects cellular growth and cell cycle

progression without causing cell death and whether the effect is specific to complex II inhibitor, we first attempted to determine subcytotoxic doses of mitochondrial respiratory inhibitors by examining PARP cleavage as a marker of apoptosis (Fig. 1A). And we decided to use 10 μM rotenone, 400 μM TTFA, 10 μM antimycin A, and 10 μM oligomycin, since these concentrations of the inhibitors displayed similar subcytotoxic effects. Interestingly, different inhibitors induced distinct morphological changes in Chang cells, immortalized human hepatocytes, which have recently been employed to develop stress-induced cellular senescence in our laboratory [Yoon et al., 2002, 2003]. With rotenone, the cells became long and oval shaped; with TTFA, the cells were shaped like sharp tripods; with antimycin A, cells became smooth triangles; and with oligomycin, cells were shaped like polygons (Fig. 1B). In addition, the inhibitors had distinct effects on cell cycle progression in an asynchronous population of cells (Fig. 1C). Rotenone arrested

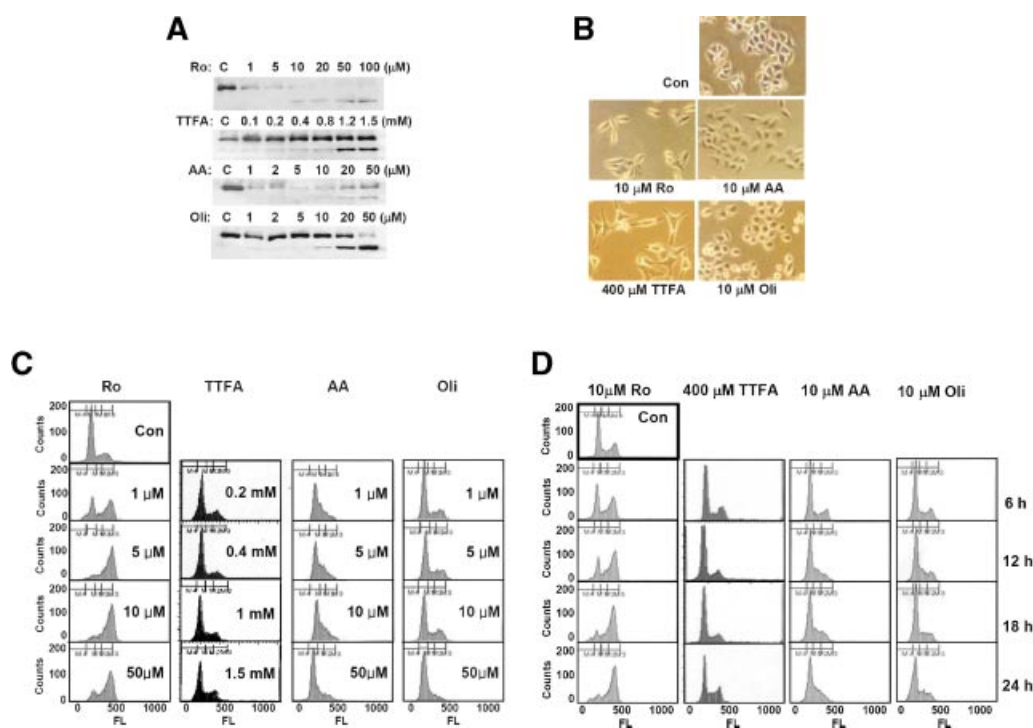


Fig. 1. Diverse effects of mitochondrial respiratory inhibitors on cellular morphology and cell cycle progression. Chang cells were stimulated with the indicated final concentration of rotenone (Ro), 2-thienyltrifluoroacetone (TTFA), antimycin A (AA), and oligomycin (Oli) for 18 h. **A:** Western blot analysis with PARP antibody (C2-10, Zymed Lab.) to monitor cleavage status of PARP as a marker for apoptosis. **B:** Cellular morphology was

visualized after treatment with the indicated dose of the inhibitors for 18 h. **C:** Cell cycle distribution of the cells exposed to the inhibitors were examined by flow cytometric analysis after staining the cells with PI. **D:** Time-dependent changes of cell cycle distribution by the subcytotoxic doses of mitochondrial inhibitors. [Color figure can be viewed in the online issue, which is available at www.interscience.wiley.com.]

Chang cells at the G2/M phase in a dose-dependent manner, cells challenged with antimycin A slowly accumulated at the G1 and S phases, and a subset of oligomycin-treated cells were arrested at the G1 phase at a high concentration of oligomycin. Similar effects were observed over a 24-h period when cells were exposed to subcytotoxic doses of the inhibitors (Fig. 1D). Surprisingly, TTFA did not cause a marked change in cell cycle distribution, indicating that complex II inhibition does not affect any specific phase of the cell cycle (Fig. 1C,D). These results further suggest that respiratory inhibitors that specifically inhibit electron transfer at the five complexes might act via distinct mechanisms and signaling pathways to affect cell cycle progression; consequently, they may achieve this effect via different pathways although the final effect on respiration and ATP generation is the same with all of the inhibitors.

TTFA Induces Mitochondrial Dysfunction and Slows the Cellular Growth Rate Without Cell Death

Although complex II inhibition by TTFA did not affect cell cycle distribution in an asynchro-

nous population, the cellular growth rate was significantly diminished without showing dead cells (Fig. 2A). Only after 3 days of treatment was there minor appearance of cell death observed, as assessed by the trypan blue exclusion assay (data not shown). To confirm the effect of TTFA on mitochondrial respiration, 400 μ M TTFA was directly added to the respiring Chang cells in a Mitocell chamber. This subcytotoxic dose of TTFA lowered the cellular oxygen consumption rate to 67% of control (Fig. 2B), disrupted the mitochondrial membrane potential, and induced morphological fragmentation (Fig. 2C,D). These results indicate that partial mitochondrial dysfunction triggered by 400 μ M TTFA decreases the cellular growth rate without causing cell death.

Complex II Inhibition Induces an Overall Delay in Cell Cycle Progression That is Associated With p21^{CIP1} Induction

To elucidate how the cellular growth rate is diminished without induction of cell death or cell-cycle arrest at any specific phase, we added 400 μ M TTFA to Chang cells that were synchronized in late G1 phase by double

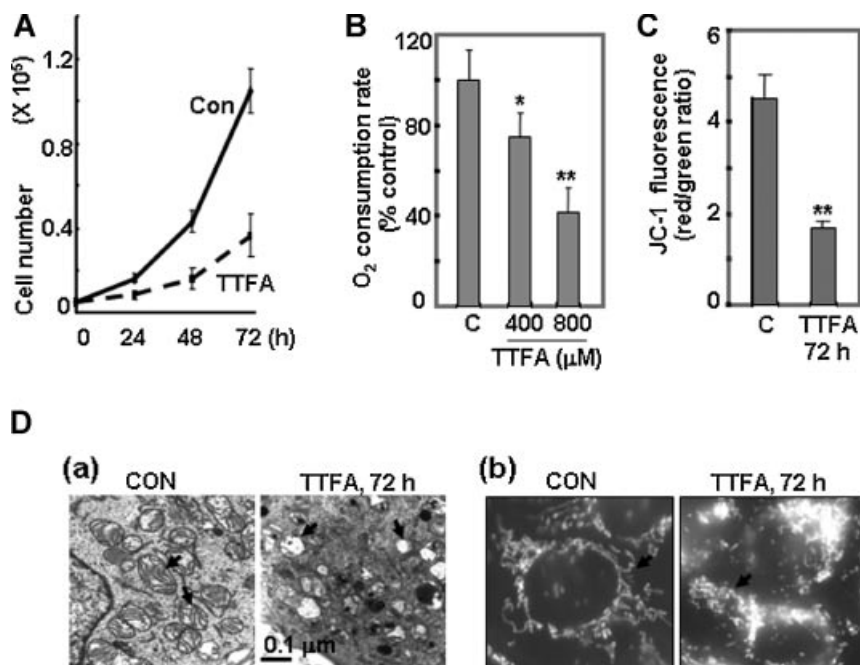


Fig. 2. Decreased cellular growth rate and mitochondrial dysfunction by complex II inhibition. **A:** Cellular growth rate was monitored by counting the trypan blue-excluded cells at the indicated time after treated with 400 μ M TTFA. **B:** Direct inhibition of cellular respiration by TTFA was examined with Mitocell equipped with Clark oxygen electrode as described in "Materials and Methods". **C:** Mitochondrial membrane potential

was monitored by comparing the ratio of red fluorescence intensities (active mitochondria) to green ones (inactive mitochondria) of JC-1-stained cells. **D:** EM images of Chang cells (a) and fluorescence images of mitochondrial morphology of mtRFP-Chang cells (b) were obtained as described in "Materials and Methods." Arrows indicate mitochondria (* P < 0.05; ** P < 0.01 vs. control).

thymidine treatment. When the cells were collected at 6-h intervals, the time required for returning to G1 phase was delayed from 18 h (control cells) to nearly 30 h (TTFA-treated cells) (Fig. 3A). To determine the effect of TTFA on each phase of the cell cycle, the TTFA-treated synchronized cells were monitored at 2-h intervals. Surprisingly, the time that cells spent in each phase (G1, S, and G2/M) was 1.5 to 1.6 times greater than in control cells; this time was estimated by determining how long it took for cells to be distributed at each phase (Fig. 3B; indicated with horizontal bars below the graph). Control and TTFA-treated cells showed the greatest difference in their cell distribution patterns at 18 h. At this time point, TTFA-treated cells displayed 16% of total cell population at G1, 23% at S, and 55% at G2/M phase, whereas control cells showed 77% at G1, 13% at S, and 7% at G2/M phase (indicated with arrows in Figs. 3A,B). The delayed effect was also dose-dependent, as evidenced by the delayed return of the synchronized cells into G1 phase 18 h after exposure to TTFA (Fig. 3C).

We next examined expression of the cell cycle regulators p16^{INK4A}, p21^{CIP1}, and p27^{KIP1} in TTFA-treated cells. Expression of p21^{CIP1} increased in a time- and dose-dependent manner, whereas p27^{KIP1} expression was relatively constant and p16 expression decreased in a time- and dose-dependent manner. This suggested that p21^{CIP1} is involved in the observed delayed cell cycle progression (Fig. 3D). These results suggest that complex II inhibition by TTFA delays the progression of all cell cycle phases, and that this delay may involve or be mediated by p21^{CIP1}.

Elevation of Intracellular ATP Partially Reverses the TTFA-Induced Delay in Cell Cycle Progression

To better understand the delayed cell cycle progression observed in TTFA-treated cells, we wished to identify the major intracellular mediator(s) of this phenomenon. A mitochondrial complex II defect would be expected to affect cellular ATP levels. We therefore monitored the intracellular ATP level after complex II inhibition. In the first 36 h after exposure to 400 μ M TTFA, the intracellular ATP level only decreased slightly; this decrease was not significant (Fig. 4A). However, at 48 h, a marked decline in the ATP level was observed. To establish whether the early (0–36 h) decline in the ATP level contributed to delayed cell cycle

progression, we used high glucose medium (HG) that was supplemented with 25 mM glucose to elevate the ATP level. Chang cells produced 1.8-fold more ATP in HG than in normal medium with low glucose (LG). The 48-h ATP level of TTFA-treated cells in HG also decreased, but the ATP level was similar to the level in control cells in LG (Fig. 4A). Cell cycle distribution was not affected by HG alone in either asynchronous or synchronous conditions (Fig. 4B,C). However, when TTFA was applied to synchronized cells in HG, the delay in cell cycle progression was partially reversed, as evidenced by an increase in the G1 population at 18 h (arrows), implying that although the slight decrease in ATP level may affect cell cycle progression, it is not the major mediator (Fig. 4C).

TTFA Triggers ROS Overproduction and Subsequent Oxidative Stress

It is well known that inhibition of mitochondrial respiration augments ROS production and oxidative stress. To determine whether ROS or oxidative stress is involved in the TTFA-induced delay in cell cycle progression, we monitored ROS and intracellular glutathione (GSH) levels as well as GSH oxidation in TTFA-treated Chang cells. Using DCF-DA and DHR123 fluorescent dyes, we observed a dose-dependent increase in intracellular ROS 15 min after TTFA addition (Fig. 5A, panels a–c). Time-dependent ROS production by TTFA showed a biphasic pattern, suggesting that two different mechanisms were involved (Fig. 5A, panel d). Biphasic variation similar to that of ROS production was also observed for GSH oxidation when we monitored GSSG production, which may be a result of ROS production (Fig. 5B, panel a). Moreover, the total GSH level declined transiently at 12 h (Fig. 5B, panel b). These results suggest that ROS and the accompanying oxidative stress may initially mediate delayed cell cycle progression in TTFA-treated cells.

To investigate this hypothesis, we examined the effects of the antioxidants N-acetyl cysteine (NAC), GSH, and L-2-oxothiazolidine-4-carboxylic acid (OTC) on delayed cell cycle progression in TTFA-treated Chang cells. After synchronization, cells were pretreated with NAC (5 mM), GSH (2 mM), or OTC (10 mM) prior to treatment with TTFA. Cell cycle distribution was analyzed at 18 h. All three antioxidants (NAC, GSH, and OTC) protected the cells against the TTFA-induced delay (Fig. 5C,D). Amazingly, 56.2% of

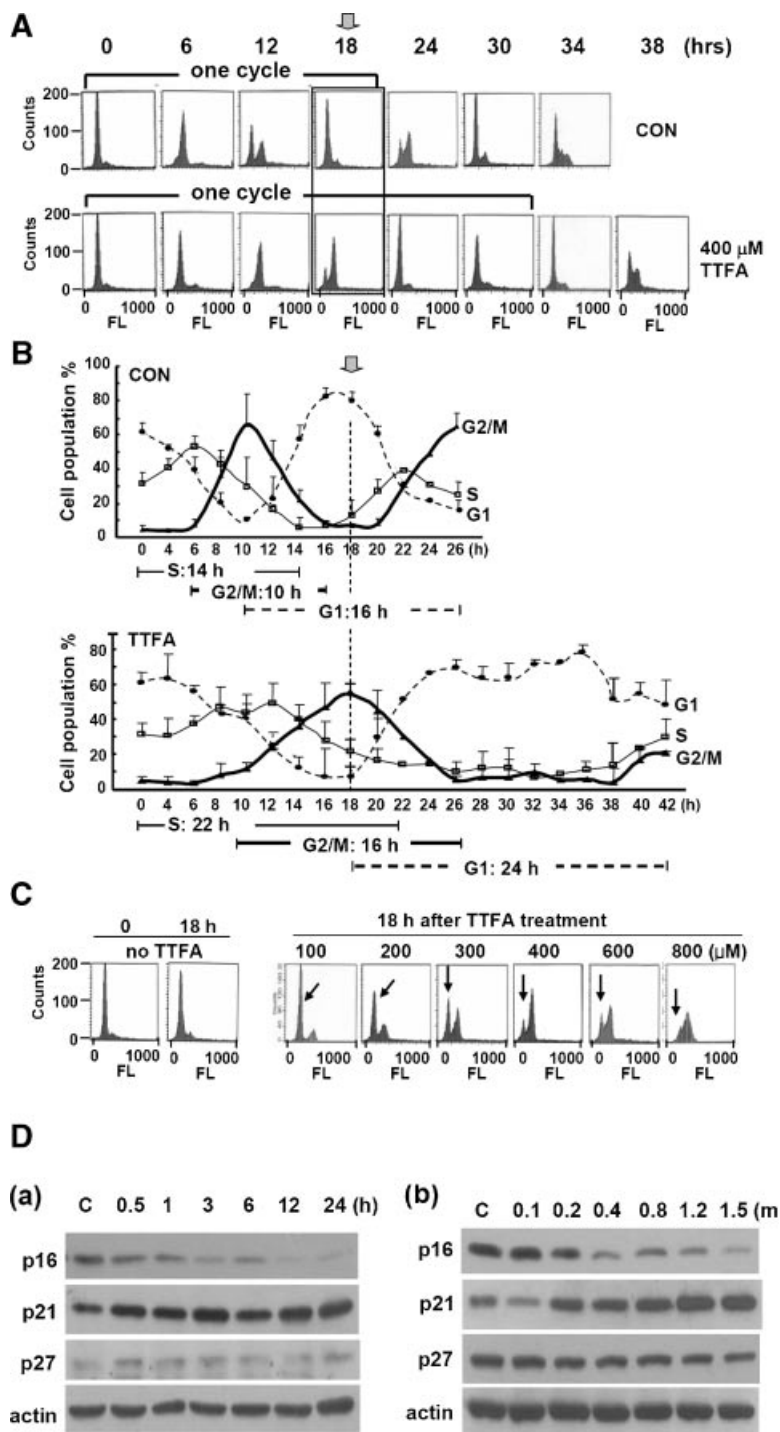


Fig. 3. Overall delay in cell cycle progression by TTFA. Chang cells were synchronized by double-thymidine block (DTB) and refreshed with DMEM media in the absence or presence of TTFA. At the indicated times, the cells were collected by trypsinization and stained with PI for flow cytometric analysis. **A:** Cell cycle distribution of the cells released from the synchronization in the absence (CON) or presence of 400 μ M TTFA at the indicated time. **B:** Cell population (%) in each phase (G1, S, G2/M) of the cell cycle of the released cells was obtained at the indicated time. The time required for one cycle of each phase was

roughly estimated and indicated in the bottom of the graph. **C:** Cell cycle distribution of the synchronized cells 18 h after release with the indicated final concentration of TTFA for 18 h. Arrows indicate cell population at the G1 phase. **D:** Chang cells were exposed to 400 μ M TTFA for the indicated time periods (a) or exposed to the indicated concentration of TTFA for 18 h (b). The cell lysates were subjected to Western blot analysis with antibodies against p27^{KIP1} (clone 57, BD Transduction, KY), p21^{CIP1} (C-17, Santa Cruz Biotech.), and p16^{INK4A} (G175-1239, BD PharMingen, CA).

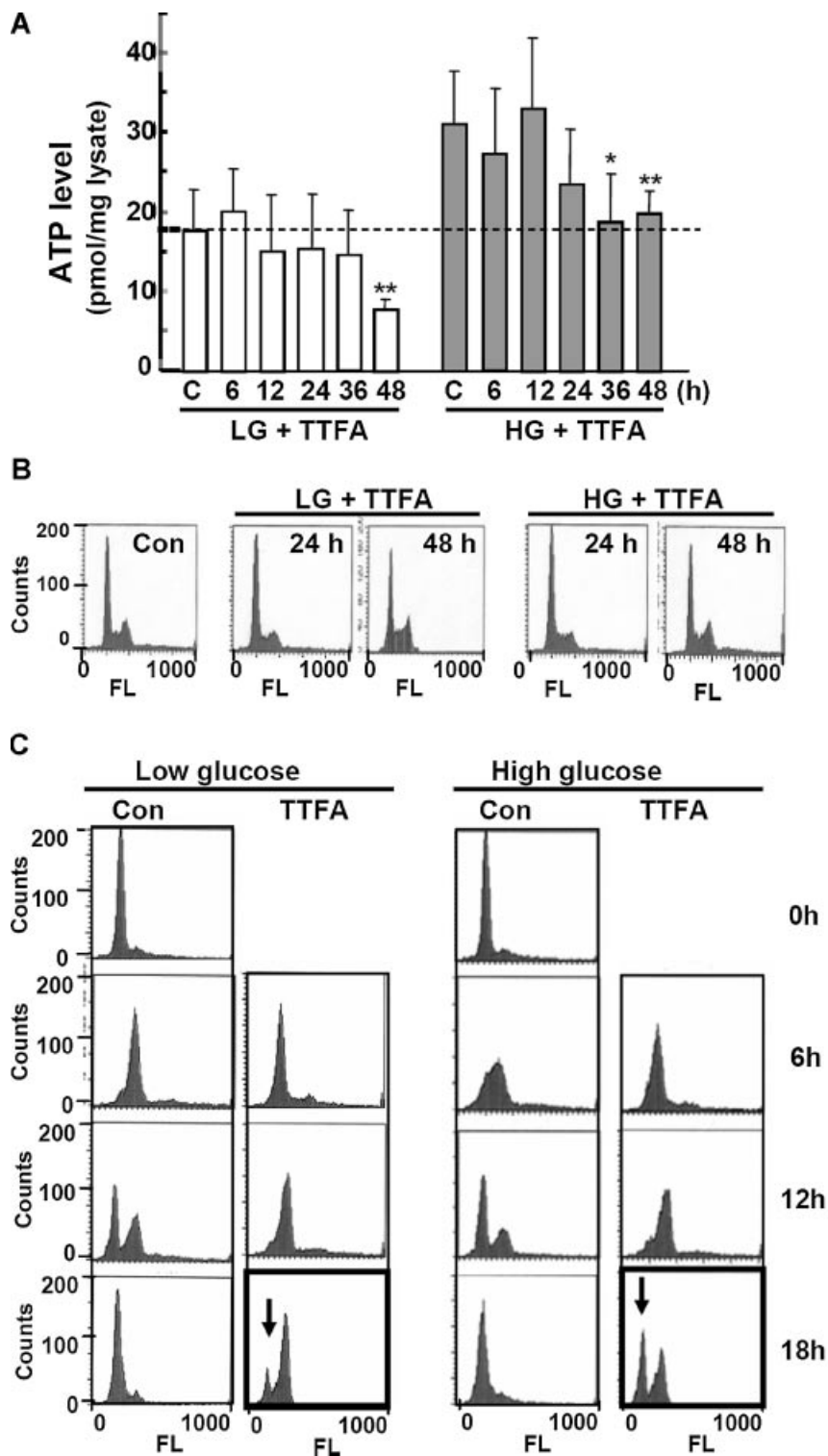


Fig. 4. Elevation of cellular ATP level with high glucose media partially reversed the TTFA-induced cell cycle delay. Chang cells were exposed to 400 μ M TTFA in low glucose (LG) or high glucose (HG) media in an asynchronous condition or after synchronization by DTB. **A:** After the indicated periods, the asynchronous Chang cells were harvested and the lysates were assayed for total intracellular ATP level. **B:** Cell cycle distribution of asynchronous Chang cells was examined by flow cytometric analysis after staining the cells with PI. **C:** Cell cycle progression of the synchronized Chang cells was monitored with intervals of 6 h. Arrows indicates cell population at the G1 phase (* $P < 0.05$; ** $P < 0.01$ vs. control).

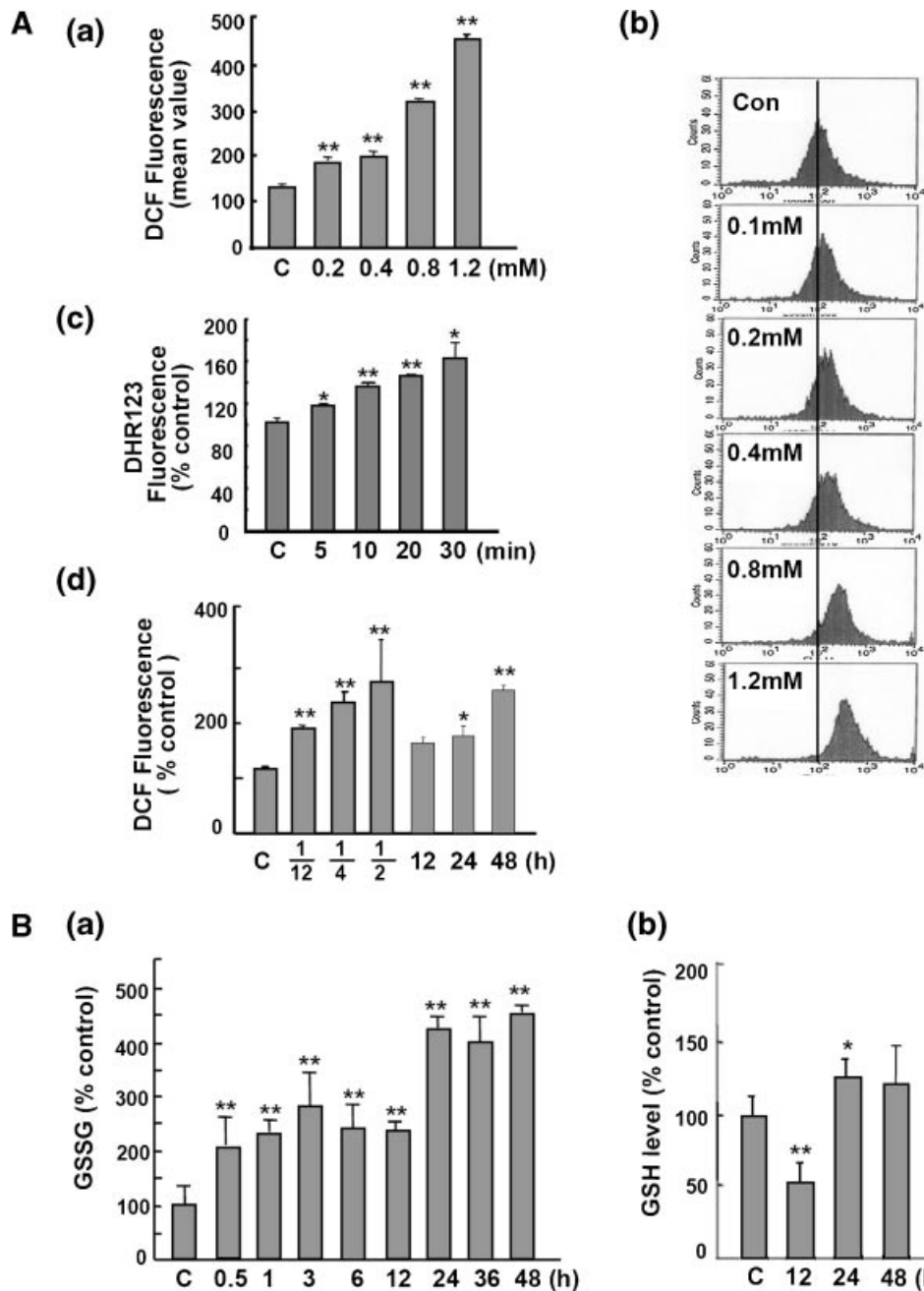


Fig. 5. The delayed cell cycle progression by complex II inhibition was mainly due to ROS overproduction. **A:** Chang cells were treated with the indicated concentration of TTFA for 15 min (**a,b**) or treated with 400 μ M for the indicated time period (**c,d**). The cells were stained with DCF-DA or DHR123 and applied to flow cytometry for the analysis of intracellular ROS level as described in "Materials and Methods." Average mean values are shown in (a) and its representative fluorescence distributions by flow cytometric analysis are in (b). c,d were presented as percent of control. **B:** Chang cells were treated with 400 μ M for the indicated time period and applied to monitor the oxidized GSSG levels (a) and total GSH levels (b). Total GSH concentration was

118.5 pmol/ μ g lysate and oxidized GSSG concentration was 0.76 pmol/ μ g lysate in control Chang cells. **C,D:** Chang cells were synchronized by DTB and pretreated with NAC, GSH, OTC, and then released from the synchronization for 18 h with media containing 400 μ M TTFA in the absence or presence of the antioxidants. C: Cell cycle distribution was examined by flow cytometric analysis after staining the cells with PI. Representative patterns are shown. D: Total GSH levels of Chang cells after exposed to 10 mM OTC for 12 h (a). The cell population at G1 phase shown in (C) was quantitated and expressed as percent of control (b). Arrows indicate cell population at the G1 phase (* P <0.05; ** P <0.01 vs. control).

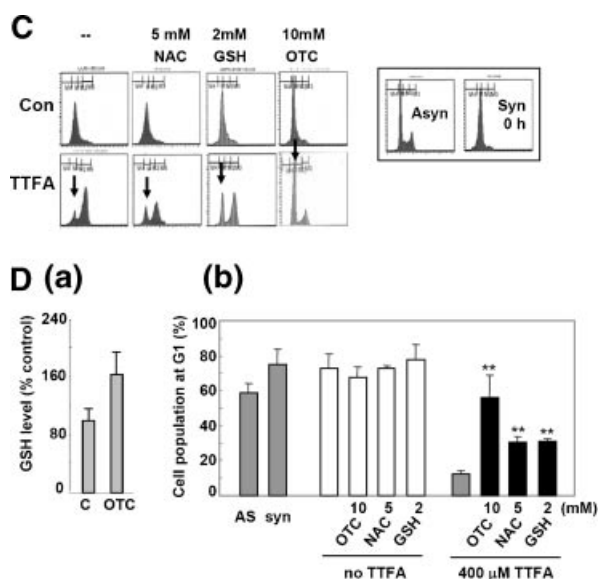


Fig. 5. (Continued)

TTFA-treated cells returned to G1 phase when pretreated with 10 mM OTC; this is an 83% recovery compared to the G1 population in the control cell population, and led to a significant increase in intracellular GSH (Fig. 5D, panel a). In contrast, 67.8% of control cells (OTC only) and 12.3% of TTFA-treated cells without OTC were in G1 phase (Fig. 5D, panel b). These results suggest that ROS generated by TTFA lead to the observed delay in cell cycle progression, and that elevation of intracellular GSH by OTC can effectively prevent this delay.

DISCUSSION

Mitochondrial complex II defects have recently become a focus of research due to their possible roles in ageing, cancer, and neuromuscular disorders such as Huntington's disease, myopathy, and encephalopathy [Liu et al., 1996; Ishii et al., 1998; Baysal et al., 2000; Sugimoto et al., 2000; Rustin and Rotig, 2002; Benn et al., 2003; Benchoua et al., 2006]. However, the role that complex II defects play in these diseases remains unknown. In this study, we aimed to elucidate how complex II defects contribute to cellular growth control associated with senescence and ageing by using TTFA, a conventional complex II inhibitor. Here, we demonstrate that TTFA decreases the cellular growth rate *in vitro*, but has no clear effects on cell cycle distribution in asynchronous conditions (Fig. 1). Detailed examination of cells

synchronized at late G1 followed by TTFA treatment reveals that TTFA delays overall cell cycle progression; this is a unique phenomenon that is not observed with other mitochondrial complex inhibitors (Fig. 3). These observations are consistent with our previous report that the complex II inhibition by deferoxamine, an iron chelator, also delayed overall cell cycle progression [Yoon et al., 2003]. In addition, the complex I inhibitor, rotenone, induced cell cycle arrest at G2/M, a complex III inhibitor induced slow accumulation at G1 and S phases, and oligomycin resulted in substantial accumulation of cells at G1 in asynchronous cells (Fig. 1). These diverse results were also similarly obtained in the synchronized cells (data not shown). Similar observations with the respiratory inhibitors except TTFA have been reported using different cell lines, but it was not quite clear whether the effects were due to complex-specific inhibition or if they were cell-type specific [Loffler, 1985; Sweet and Singh, 1995; Nishimura et al., 2001; Gemin et al., 2005]. Our results clearly indicate that the overall delay in cell cycle progression is quite specific to the complex II inhibitor and that all the four respiratory complex inhibitors have their own specific effects on cell cycle progression via distinct mechanisms and signaling pathways although the final effect on respiration and ATP generation is the same with all of the inhibitors. Another diverse effect of the respiratory inhibitors was displayed on cellular morphology (Fig. 1A). Cellular shape is mainly maintained by balanced reorganizing activity (polymerization and its direction) of cell cytoskeleton proteins, such as actin and tubulin. Importance of intracellular ATP level in reorganization of cell cytoskeleton [Maro and Bomens, 1982; Kats and Wals, 1987] and a direct action of rotenone in microtubule assembly have been noticed [Srivastava and Panda, 2007]. In addition, ROS is known to regulate actin cytoskeleton [Moldovan et al., 2006]. Based on these informations, we speculate that the respiratory inhibitors may also affect cytoskeleton reorganization differentially through different microenvironmental control of cellular ATP and ROS levels, or their unknown specific action on cytoskeleton.

The data in this study demonstrate that each respiratory complex modulates a specific signaling pathway that affects cell cycle progression. When we examined whether any specific cell cycle regulator is involved in the delayed cell

cycle progression, a time- and dose-dependent decrease of p16^{INK4A} expression was observed in addition to p21^{CIP1} induction (Fig. 3D). p16^{INK4A} inhibits cyclinD/CDK4/6 complex formation, thereby inhibiting the G1-S transition and subsequently arresting cells at the G1 phase; however, p21^{CIP1} inhibits the activity of cyclin E/CDK2, cyclin A/CDC2, and cyclin B/CDC2 complexes, indicating that p21^{CIP1} inhibits all phases of the cell cycle [Sherr and Roberts, 1999]. Therefore, it seems reasonable to hypothesize that suppressing expression of p16 would prevent specific arrest at the G1 phase and that inducing p21^{CIP1} expression would affect all phases of the cell cycle to a similar degree; however, further studies are needed to confirm this.

What is the major mediator of TTFA-induced delayed cell cycle progression? As mentioned earlier, ROS production and decreased ATP generation are phenomena that are typically accompanied by mitochondrial respiratory defects. Our results confirmed that complex II inhibition by TTFA slowly decreased cellular ATP levels and caused a biphasic increase in ROS levels. We also demonstrated that ROS production caused by TTFA is the major factor involved in delayed cell cycle progression, while decreased ATP generation also affects this process to a lesser extent (Figs. 4 and 5). Complexes I and III are well-known sites for superoxide generation [Isenberg and Klaunig, 2000; Miwa and Brand, 2005; Grivennikova and Vinogradov, 2006], whereas the involvement of complex II in ROS generation is not recognized well. The structure of complex II was determined with TTFA in the ubiquinone binding sites by X-ray crystallography [Sun et al., 2005], and in vitro direct production of superoxide by complex II has recently been reported [Yankovskaya et al., 2003]. The most reliable evidence for in vivo ROS production by complex II defects is that a mutation in succinate dehydrogenase causes superoxide anion production and ageing [Ishii et al., 1998; Senoo-Matsuda et al., 2001], in agreement with our findings. Among the antioxidants used in this study, OTC, a cysteine precursor and substrate of glutathione synthase [Lee et al., 2004], was the most effective in preventing the TTFA-induced delay in cell cycle progression by augmenting the intracellular GSH level (Fig. 5). If ROS overproduction is common to all respiratory complex defects, then how does ROS generated by TTFA

specifically modulate the cell cycle? Notably, individual respiratory inhibitors display distinct time courses and dose-dependent ROS production levels (Supplementary Fig. 1). Therefore, the microenvironment, timing, and magnitude of ROS production caused by different inhibitors may have different impacts on cell cycle progression via activation of specific signaling pathways. Although limited information on the effects of complex II inhibition by TTFA on signaling modulation is available, several recent studies describes that complex II inhibition by 3-nitropropionic acid (3-NPA) increases mitochondrial superoxide generation [Bacsi et al., 2006] and subsequently activates redox-sensitive JNK and p38 MAPK in response to the ROS [Hsieh and Papaconstantinou, 2002; Hsieh et al., 2003]. Moreover, the stress-activated protein kinases p38 and JNK stabilize p21^{CIP1} protein [Kim et al., 2002]. Therefore, we could suggest a working hypothesis that complex II inhibition delays cell cycle progression by p21^{CIP1} induction through activation of p38 or JNK in response to ROS generation.

Our results demonstrate that complex II defects induce an overall delay in cell cycle progression by affecting all phases of the cell cycle, and that this effect is predominantly due to ROS production and the accompanying oxidative stress. In addition, we report that elevation of intracellular GSH using OTC is the most effective method for preventing the progression delay. Finally, we propose that the delayed cell cycle progression caused by a complex II defect may contribute to ageing and degenerative diseases by suppressing cellular growth and proliferation without arresting cells at any specific cell cycle phase.

REFERENCES

- Albayrak T, Scherhammer V, Schoenfeld N, Braziulis E, Mund T, Bauer MK, Scheffler IE, Grimm S. 2003. The tumor suppressor *cybL*, a component of the respiratory chain, mediates apoptosis induction. *Mol Biol Cell* 14: 3082–3096.
- Armstrong JS, Hornung B, Lecane P, Jones DP, Knox SJ. 2001. Rotenone-induced G2/M cell cycle arrest and apoptosis in a human B lymphoma cell line PW. *Biochem Biophys Res Commun* 289:973–978.
- Bacsi A, Woodberry M, Widger W, Papaconstantinou J, Mitra S, Peterson JW, Boldogh I. 2006. Localization of superoxide anion production to mitochondrial electron transport chain in 3-NPA-treated cells. *Mitochondrion* 6:235–244.
- Baysal BE, Ferrell RE, Willett-Brozick JE, Lawrence EC, Myssiorek D, Bosch A, van der MA, Taschner PE,

- Rubinstein WS, Myers EN, Richard CW III, Cornelisse CJ, Devilee P, Devlin B. 2000. Mutations in SDHD, a mitochondrial complex II gene, in hereditary paraganglioma. *Science* 287:848–851.
- Benchoua A, Trioulier Y, Zala D, Gaillard MC, Lefort N, Dufour N, Saudou F, Elalouf JM, Hirsch E, Hantraye P, Deglon N, Brouillet E. 2006. Involvement of mitochondrial complex II defects in neuronal death produced by N-terminus fragment of mutated huntingtin. *Mol Biol Cell* 17:1652–1663.
- Benn DE, Croxson MS, Tucker K, Bambach CP, Richardson AL, Delbridge L, Pullan PT, Hammond J, Marsh DJ, Robinson BG. 2003. Novel succinate dehydrogenase subunit B (SDHB) mutations in familial pheochromocytomas and paragangliomas, but an absence of somatic SDHB mutations in sporadic pheochromocytomas. *Oncogene* 22:1358–1364.
- Gemin A, Sweet S, Preston TJ, Singh G. 2005. Regulation of the cell cycle in response to inhibition of mitochondrial generated energy. *Biochem Biophys Res Commun* 332:1122–1132.
- Grivennikova VG, Vinogradov AD. 2006. Generation of superoxide by the mitochondrial Complex I. *Biochim Biophys Acta Bioenerg* 1757:553–561.
- Hsieh CC, Papaconstantinou J. 2002. The effect of aging on p38 signaling pathway activity in the mouse liver and in response to ROS generated by 3-nitropropionic acid. *Mech Ageing Dev* 123:1423–1435.
- Hsieh CC, Rosenblatt JI, Papaconstantinou J. 2003. Age-associated changes in SAPK/JNK and p38 MAPK signaling in response to the generation of ROS by 3-nitropropionic acid. *Mech Ageing Dev* 124:733–746.
- Isenberg JS, Klaunig JE. 2000. Role of the mitochondrial membrane permeability transition (MPT) in rotenone-induced apoptosis in liver cells. *Toxicol Sci* 53:340–351.
- Ishiguro H, Yasuda K, Ishii N, Ihara K, Ohkubo T, Hiyoshi M, Ono K, Senoo-Matsuda N, Shinohara O, Yosshii F, Murakami M, Hartman PS, Tsuda M. 2001. Enhancement of oxidative damage to cultured cells and *Caenorhabditis elegans* by mitochondrial electron transport inhibitors. *IUBMB Life* 51:263–268.
- Ishii N, Fujii M, Hartman PS, Tsuda M, Yasuda K, Senoo-Matsuda N, Yanase S, Ayusawa D, Suzuki K. 1998. A mutation in succinate dehydrogenase cytochrome b causes oxidative stress and ageing in nematodes. *Nature* 394:694–697.
- Kats J, Wals PA. 1987. The role of ATP in the cytostructure of the hepatocytes. *J Cell Biochem* 33:127–136.
- Kim GY, Mercer SE, Ewton DZ, Yan Z, Jin K, Friedman E. 2002. The stress-activated protein kinases p38 alpha and JNK1 stabilize p21(Cip1) by phosphorylation. *J Biol Chem* 277:29792–29802.
- Lee YC, Lee KS, Park SJ, Park HS, Lim JS, Park KH, Im MJ, Choi IW, Lee HK, Kim UH. 2004. Blockade of airway hyperresponsiveness and inflammation in a murine model of asthma by a prodrug of cysteine, L-2-oxothiazolidine-4-carboxylic acid. *FASEB J* 18:1917–1919.
- Lesnefsky EJ, Hoppel CL. 2006. Oxidative phosphorylation and aging. *Ageing Res Rev* 5:402–433.
- Li N, Ragheb K, Lawler G, Sturgis J, Rajwa B, Melendez JA, Robinson JP. 2003. Mitochondrial complex I inhibitor rotenone induces apoptosis through enhancing mitochondrial reactive oxygen species production. *J Biol Chem* 278:8516–8525.
- Liu X, Kim CN, Yang J, Jemerson R, Wang X. 1996. Induction of apoptotic program in cell-free extracts: Requirement for dATP and cytochrome c. *Cell* 86:147–157.
- Loffler M. 1985. Towards a further understanding of the growth-inhibiting action of oxygen deficiency: Evaluation of the effect of antimycin on proliferating Ehrlich ascites tumour cells. *Exp Cell Res* 157:195–206.
- Maro B, Bomens M. 1982. Reorganization of HeLa cell cytoskeleton induced by an uncoupler of oxidative phosphorylation. *Nature* 295:334–336.
- Miwa S, Brand MD. 2005. The topology of superoxide production by complex III and glycerol 3-phosphate dehydrogenase in *Drosophila* mitochondria. *Biochim Biophys Acta* 1709:214–219.
- Moldovan L, Mythreye K, Goldschmidt-Clermont PJ, Satterwhite LL. 2006. Reactive oxygen species in vascular endothelial cell motility. Roles of NAD(P)H Oxidase and Rac1. *Cardiovasc Res* 71:236–246.
- Nicholls DG, Ferguson SJ. 2002. *Bioenergetics 3*. San Diego: Academic press. pp 89–216.
- Nishimura G, Proske RJ, Doyama H, Higuchi M. 2001. Regulation of apoptosis by respiration: Cytochrome c release by respiratory substrates. *FEBS Lett* 505:399–404.
- Papa S, Skulachev VP. 1997. Reactive oxygen species, mitochondria, apoptosis and aging. *Mol Cell Biochem* 174:305–319.
- Rustin P, Rotig A. 2002. Inborn errors of complex II—Unusual human mitochondrial diseases. *Biochim Biophys Acta* 1553:117–122.
- Senoo-Matsuda N, Yasuda K, Tsuda M, Ohkubo T, Yoshimura S, Nakazawa H, Hartman PS, Ishii N. 2001. A defect in the cytochrome b large subunit in complex II causes both superoxide anion overproduction and abnormal energy metabolism in *Caenorhabditis elegans*. *J Biol Chem* 276:41553–41558.
- Sherr CJ, Roberts JM. 1999. CDK inhibitors: Positive and negative regulators of G1-phase progression. *Genes Dev* 13:1501–1512.
- Srivastava P, Panda D. 2007. Rotenone inhibits mammalian cell proliferation by inhibiting microtubule assembly through tubulin binding. *FEBS J* 274:4788–4801.
- Sugimoto J, Shimohira M, Osawa Y, Matsubara M, Yamamoto H, Goto Y, Nonaka I. 2000. A patient with mitochondrial myopathy associated with isolated succinate dehydrogenase deficiency. *Brain Dev* 22:158–162.
- Sun F, Huo X, Zhai Y, Wang A, Xu J, Su D, Bartlam M, Rao Z. 2005. Crystal structure of mitochondrial respiratory membrane protein complex II. *Cell* 121:1043–1057.
- Sweet S, Singh G. 1995. Accumulation of human promyelocytic leukemic (HL-60) cells at two energetic cell cycle checkpoints. *Cancer Res* 55:5164–5167.
- Tietze F. 1969. Enzymic method for quantitative determination of nanogram amounts of total and oxidized glutathione: Applications to mammalian blood and other tissues. *Anal Biochem* 27:502–522.
- Wallace DC. 1999. Mitochondrial diseases in man and mouse. *Science* 283:1482–1488.
- Wallace DC. 2005. A mitochondrial paradigm of metabolic and degenerative diseases, aging, and cancer: A dawn for evolutionary medicine. *Annu Rev Genet* 39:359–407.

- Wolvetang EJ, Johnson KL, Krauer K, Ralph SJ, Linnane AW. 1994. Mitochondrial respiratory chain inhibitors induce apoptosis. *FEBS Lett* 339:40–44.
- Yankovskaya V, Horsefield R, Tornroth S, Luna-Chavez C, Miyoshi H, Leger C, Byrne B, Cecchini G, Iwata S. 2003. Architecture of succinate dehydrogenase and reactive oxygen species generation. *Science* 299:700–704.
- Yoon G, Kim HJ, Yoon YS, Cho H, Lim IK, Lee JH. 2002. Iron chelation-induced senescence-like growth arrest in hepatocyte cell lines: Association of transforming growth factor beta 1 (TGF- β 1)-mediated p27Kip1 expression. *Biochem J* 366:613–621.
- Yoon YS, Byun HO, Cho H, Kim BK, Yoon G. 2003. Complex II defect via down-regulation of iron-sulfur subunit induces mitochondrial dysfunction and cell cycle delay in iron chelation-induced senescence-associated growth arrest. *J Biol Chem* 278:51577–51586.
- Yoon YS, Yoon DS, Lim IK, Yoon SH, Chung HY, Rojo M, Malka F, Jou MJ, Martinou JC, Yoon G. 2006. Formation of elongated giant mitochondria in DFO-induced cellular senescence: Involvement of enhanced fusion process through modulation of Fis1. *J Cell Physiol* 209:468–480.